



HAL
open science

The cavity method for quantum disordered systems: from transverse random field ferromagnets to directed polymers in random media

Olga Dimitrova, Marc Mezard

► **To cite this version:**

Olga Dimitrova, Marc Mezard. The cavity method for quantum disordered systems: from transverse random field ferromagnets to directed polymers in random media. 2010. hal-00519376v2

HAL Id: hal-00519376

<https://hal.science/hal-00519376v2>

Preprint submitted on 23 Dec 2010

HAL is a multi-disciplinary open access archive for the deposit and dissemination of scientific research documents, whether they are published or not. The documents may come from teaching and research institutions in France or abroad, or from public or private research centers.

L'archive ouverte pluridisciplinaire **HAL**, est destinée au dépôt et à la diffusion de documents scientifiques de niveau recherche, publiés ou non, émanant des établissements d'enseignement et de recherche français ou étrangers, des laboratoires publics ou privés.



HAL Authorization

The cavity method for quantum disordered systems: from transverse random field ferromagnets to directed polymers in random media

O. Dimitrova and M. Mézard¹

¹*Laboratoire de Physique Théorique et Modèles Statistiques,
CNRS and Université Paris-Sud, Bât 100, 91405 Orsay Cedex, France*

Abstract

After reviewing the basics of the cavity method in classical systems, we show how its quantum version, with some appropriate approximation scheme, can be used to study a system of spins with random ferromagnetic interactions and a random transverse field. The quantum cavity equations describing the ferromagnetic-paramagnetic phase transition can be transformed into the well-known problem of a classical directed polymer in a random medium. The glass transition of this polymer problem translates into the existence of a ‘Griffiths phase’ close to the quantum phase transition of the quantum spin problem, where the physics is dominated by rare events. The physical behaviour of random transverse field ferromagnets on the Bethe lattice is found to be very similar to the one found in finite dimensional systems, and the quantum cavity method gets back the known exact results of the one-dimensional problem.

I. INTRODUCTION

The cavity method has been developed to study classical frustrated spin systems: spin glasses. In recent years its range of application has broadened a lot as it was applied with some success to hard computer science problems and also to some quantum problems. This paper aims at giving some background on the cavity method, both classical and quantum, and explaining how it can be used to study a quantum problem, a ferromagnetic spin system in a random transverse field, following the recent work of [1,2]. This is a problem which has been studied a lot in one dimension; we analyze it here using the cavity method which is a mean-field type method better suited for large dimensional systems. However we find that the physics is rather similar to the one found in the one-dimensional case, in the sense that rare events (rare sites with anomalously small transverse fields) play a major role in the neighborhood of the quantum critical point. This leads to very large spatial fluctuations of the spontaneous magnetization in the ferromagnetic phase, and a broad distribution of the local magnetic susceptibilities in the paramagnetic phase. These effects, which are typical of the ‘Griffiths phase’ described in low dimensions, are found here through the use of an auxiliary problem of directed polymers in random media: the rare-event dominated regime of the ferromagnetic-paramagnetic phase transition is related to the glass transition of the polymer problem.

This paper is organized as follows. Sec.II gives an introduction to the cavity method in classical spin systems. Sec.III defines the random transverse field ferromagnet and gives some background on this problem. The naive mean field approach to this problem is explained in Sec.IV. Sec. V introduces the quantum cavity method and discusses some systematic approximation schemes which can be used in this context. These approximation schemes are tested in Sec.VI by applying them to a very simple, and very well understood, problem: the pure ferromagnet in a transverse field. Sec.VII describes the use of the quantum cavity method, with a ‘cavity-mean-field’ approximation, to study the phase diagram of a ferromagnet in a random transverse field. It derives the phase transition line in the plane disorder-temperature, and describes the main properties of the low-temperature ferromagnetic and paramagnetic phases, in particular the large fluctuations of the order parameter and of the susceptibility. This section ends by a study of the one-dimensional case, where the cavity method gets the known exact results, and a discussion of the higher-dimensional

cases, for which the Bethe lattice analysis provides a useful mean-field approximation. A short summary is given in Sec.VIII.

II. THE CLASSICAL CAVITY METHOD

A. The Sherrington-Kirkpatrick model

The cavity method has been introduced twenty five years ago in the context of spin glass mean field theory³. The solution of the fully connected Sherrington-Kirkpatrick (SK)⁴ model had been found a few years before by G. Parisi⁵, who had proposed, within the replica approach, an inspired Ansatz of replica symmetry breaking (RSB). The cavity method gave an alternative solution, with identical physical content and results to the replica approach, but which was much more transparent. Instead of the mysterious replicas, it used a purely probabilistic approach, based on three assumptions which had been found to be hidden in the form of Parisi's RSB Ansatz: the existence of many pure states⁶, ultrametricity⁷, and the exponential distribution of free energies of the pure states⁸. This approach has turned out to be very powerful and has served as a starting point of recent works by Talagrand⁹ and Guerra¹⁰ which established rigorously the exactness of the free energy obtained by the RSB/cavity method (although the ultrametric property has still not been proven).

In a nutshell, the cavity method as it was applied to the SK model consists in assuming some structure for a N -spin system s_1, \dots, s_N , and checking self consistently that this structure is reproduced when one adds a new spin s_0 and goes to a $N + 1$ spin-system. Within the simplest replica symmetric (RS) approximation, the main assumption is that the correlation functions are small. The local field on s_0 then has a Gaussian distribution, with a width which must be reproduced self-consistently and gives the Edwards-Anderson order parameter¹¹. This approach gives the RS solution, which is correct at temperatures above the de-Almeida Thouless (AT) line¹². It breaks down in the spin glass phase, when the proliferation of pure states induces a non-trivial correlation between distinct spins. In order to study the spin glass phase, one must explicitly assume the existence of many pure states^{13,14} with free energies distributed as a Poisson process with exponential distribution³. Within each state, the correlations are small and the cavity method can be applied. But the addition of the new spin s_0 creates a free energy shift which depends on the state: the

free energies are reshuffled, and the selection of low free energy states (by the Boltzmann weight) biases the local field distribution. The whole cavity RSB approach relies on controlling these crossings of the free energies of the states, and checking the self consistency of the basic hypotheses. The results are exactly identical to those of the replica approach.

B. Finite connectivity spin glasses

It was soon realized that it would be very instructive to go beyond the SK model by studying spin glass models in which each spin has only a finite number of neighbours. In order to introduce mean field models with this property, the usual approach is to study the Bethe lattice, which is usually defined as the interior of a Cayley tree: taking a large Cayley tree of depth M , one studies the interior part up to depth L . The Bethe lattice is then defined by the double limit $\lim_{L \rightarrow \infty} \lim_{M \rightarrow \infty}$ (see Fig. 1). This procedure is fine for ferromagnetic interactions, but it raises a problem when one studies spin glasses where a crucial ingredient is the frustration due to loops in which the product of exchange couplings is negative. A simple procedure is to induce frustration by fixing randomly (or imposing some type of local fields on) the spins at the boundary of the tree. However most of the physics is then put by hand through this boundary condition, which involves a finite fraction of the total number of spins. For instance fixing the boundary spins to ± 1 independently with probability $1/2$ ^{15,16} gives a system which does not have a genuine spin glass phase (technically it is always replica symmetric). It has been found recently how the boundary conditions should be fixed in order to get RSB: the correct procedure involves the process of broadcast and reconstruction¹⁷ and creates subtly correlated boundary fields.

An alternative construction is to define the Bethe lattice spin glass through a random regular graph, taken uniformly from all the graphs where each spin has $K+1$ neighbours (see Fig. 1). Large random regular graphs with $K \gg 1$ vertices have a locally tree-like structure like the interior of a Cayley tree, as the typical size of a loop is of order $\log N / \log K$. These large loops create the frustration without having to play with boundary conditions. The study of spin glasses on random graph with a finite connectivity started with Viana and Bray¹⁸. The solution of spin glasses on random regular graphs within the RS approximation was found relatively early¹⁸⁻²⁰, but it took fifteen more years to understand how to handle RSB effects²¹, and this has been done so far only at the level of one, or at most two, steps of

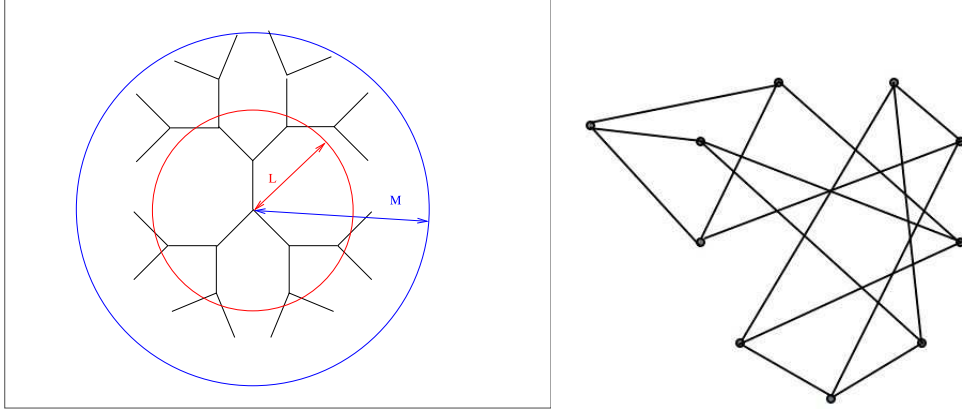


FIG. 1. Left: the usual construction of the Bethe lattice. Right: a (small) random regular graph. The local structure in large random regular graph is tree-like, as in the center of a Bethe lattice.

RSB. Here we shall briefly review how the cavity method can be used to study this problem, mostly at the RS level, as this gives the building blocks of the quantum cavity method which we use below.

Let us study the equilibrium properties, at inverse temperature β , of a general Ising spin glass problem with a random field on a Bethe lattice, defined by the Hamiltonian

$$H = - \sum_{\langle ij \rangle} J_{ij} s_i s_j - \sum_i B_i s_i \quad (1)$$

where $\langle ij \rangle$ are the links of a random-regular graph of degree $K + 1$. The idea is to use the local tree-like property for rooted trees. Let us pick up one spin, say s_0 , and delete the edge between 0 and one of its neighbours. Up to any finite distance, s_0 is now the root of a tree. Let us denote by h_0 the local 'cavity' magnetic field on the root s_0 due to this tree, so that $\langle s_0 \rangle = \tanh(\beta h_0)$. Denote by s_1, \dots, s_K its neighbours on the tree, and by h_1, \dots, h_k their cavity fields (so that for instance the magnetization of s_1 in the absence of s_0 is $\tanh(\beta h_1)$). The Boltzmann measure on s_0 is then

$$P(s_0) = \frac{1}{Z_0} \sum_{\{s_i\}} \exp \left(\beta \left[B_0 s_0 + \sum_{i=1}^K (J_{0i} s_0 s_i + h_i s_i) \right] \right) \quad (2)$$

By doing explicitly the sum over the spins s_i , one gets the recursion

$$h_0 = B_0 + \frac{1}{\beta} \sum_{i=1}^K \operatorname{atanh}(\tanh(\beta J_{0i}) \tanh(\beta h_i)) \quad (3)$$

which is illustrated pictorially in Fig.2. One way to describe it is to build the tree rooted in s_0 by considering the K trees rooted on s_1, \dots, s_K (in absence of s_0) and merging them.

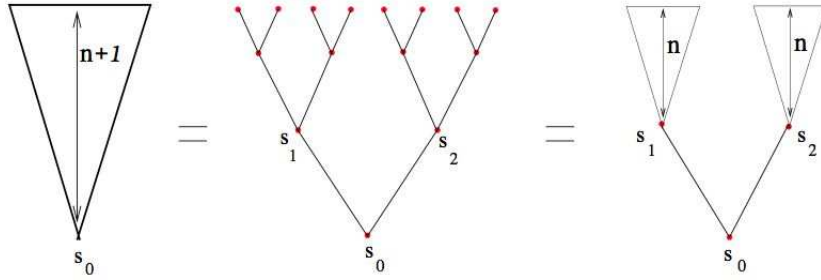


FIG. 2. The recursion relation for the local magnetic field on the root of a rooted tree, here for the case $K = 2$.

These recursion ‘cavity’ equations are always correct on a tree. On a random regular graph they are correct whenever the joint probability of the spins s_1, \dots, s_K in the absence of s_0 factorizes into a product $\prod_i \exp(\beta h_i s_i) / (2 \cosh(\beta h_i))$. Two conditions are needed for this absence of correlations of neighbouring spins. One is the local tree-like property which guarantees that any two neighbouring spins s_i, s_j , with $i, j \in \{1, \dots, K\}$, are far away on the graph obtained by eliminating the site s_0 and all edges connected to it. The second one is that the correlations decay at large distance, so that the correlations between two neighbours s_i and s_j (which are typically at distance $\log N / \log K$ when s_0 is absent), vanish in the large N limit. This is true when the system is in its paramagnetic phase. It is not correct in a ferromagnetic phase or in a spin glass phase because long-range correlations develop. However, if one is able to restrict the measure to one single pure state (where by definition correlations decay at large distance), then the recursion relations are correct.

These recursion relations can be used in two main ways:

1- On a given sample, one can see these equations as a set of self-consistent equations relating cavity fields: there are two such cavity fields for each edge $\langle ij \rangle$ of the graph, one is the field on site i in the absence of j (case where i has been chosen as root), the other one is the field on site j in absence of i . All these fields are related by the cavity equations. In the large K limit these equations reduce to the ‘TAP’ equations¹³. These RS cavity equations are also well known in computer science under the name of ‘belief propagation’ equations²².

2- One can also study the statistics of cavity fields. Suppose that the local magnetic fields B_i are independent random variables drawn from a distribution $P_{ext}(B)$, and the exchange couplings are independent random variables drawn from a distribution $\rho(J)$. At the RS

level, one expects a single solution for all cavity fields on a given instance. Then one can define the distribution of cavity fields $P(h)$ when one picks up an oriented edge randomly. This is the natural order parameter for this problem. Its knowledge provides the full solution of the problem when the RS hypothesis is correct. Technically, finding $P(h)$ is usually done by a ‘population dynamics’ method first introduced in [23], and developed in the present context by [21]. Its idea is the following. The update equation (3) induces a self-consistency equation for $P(h)$ which can be written as:

$$P(h) = \int dB P_{ext}(B) \prod_{i=1}^K \int dh_i P(h_i) dJ_i \rho(J_i) \delta \left(h - B - \frac{1}{\beta} \sum_{i=1}^K \operatorname{atanh}(\tanh(\beta J_i) \tanh(\beta h_i)) \right) \quad (4)$$

The population dynamics method represents $P(h)$ by a population of $M \gg 1$ fields h_1, \dots, h_M . This population is updated by a Monte-Carlo-type process in which, at each iteration, one does the following operations:

- Choose K indices $r_1, \dots, r_K \in \{1, \dots, M\}$ randomly uniformly.
- Generate K independent couplings J_1, \dots, J_K from $\rho(J)$, and a field B from $P_{ext}(B)$.
- Compute $h = B + \frac{1}{\beta} \sum_{i=1}^K \operatorname{atanh}(\tanh(\beta J_i) \tanh(\beta h_{r_i}))$
- Choose an index $j \in \{1, \dots, M\}$ randomly uniformly, and replace in the population the value h_j by the new value h .

The convergence of this method when the number of iterations is large enough can be checked by monitoring for instance moments of $P(h)$ (the r -th moment is evaluated as $(1/M) \sum_{i=1}^M h_i^r$). If M is large enough the population will give a good approximation of $P(h)$.

Note that the RSB situation is much more complicated: on a given instance there are many solutions to the system of equations relating the cavity fields. On a given oriented edge (say looking at the cavity field on i in absence of j) the cavity field can take many values depending on the solution one takes. Doing the statistics over all solutions defines a distribution of fields on each oriented edge, and the order parameter is the distribution of these distributions when one picks an edge at random. In the following quantum problems we shall use only the RS version.

III. RANDOM TRANSVERSE-FIELD FERROMAGNETS

The problem of ferromagnets in random transverse fields has received a lot of attention in recent years. These systems provide relatively simple examples of disordered systems displaying a quantum phase transition²⁴. They are described by the Hamiltonian:

$$H_F = - \sum_i \xi_i \sigma_i^z - \sum_{(ij)} J_{ij} \sigma_i^x \sigma_j^x . \quad (5)$$

where σ^z, σ^x are Pauli matrices. The exchange couplings are independent ferromagnetic interactions drawn from a distribution $\rho(J)$ which has support on $J > 0$, and the random transverse fields are independent variables drawn from a distribution $\pi(\xi)$. The lattice structure is described by the set of pairs (ij) which appear in the above sum; we suppose that this lattice is homogeneous, and each spin has exactly $z = K + 1$ neighbours. For definiteness we shall use a model where the distribution of couplings and fields are given by:

$$\rho(J) = \frac{K}{2} \theta(J) \theta(2/K - J) \quad ; \quad \pi(\xi) = \frac{1}{h} \theta(\xi) \theta(h - \xi) , \quad (6)$$

where θ is the Heaviside function. The choice of the width of the J distribution fixes the energy scale such that the mean-field critical temperature in absence of disorder has $T_c = 1$. The Hamiltonian H_F thus depends on a single parameter h which measures the degree of disorder.

The one dimensional case, which is intimately related to the two-dimensional classical model of MacCoy and Wu²⁵, has been solved in great detail by Fisher²⁶ using the strong disorder Ma-Dasgupta-Hu decimation procedure²⁷. This solution has emphasized the importance of Griffiths singularities, which manifest themselves most notably in the fact that the average susceptibility differs from the typical one. The method itself has a broad range of applications³⁰. These results have been confirmed numerically^{28,29}, and numerical simulations of the same problem in dimension two, both through the strong disorder decimation and through Monte-Carlo simulations, also point to the same kind of physics as in one dimension³¹⁻³⁵. Recent results also find the same behaviour in dimension three and higher³⁶

Using the method introduced in [1,2], we shall now study the Bethe approximation for the random transverse-field ferromagnet described by (5). We thus assume that the spins are on the vertices of a random regular graph of degree $z = K + 1$ and we want to study the phase diagram of this problem as function of the temperature T and the amount of disorder h .

IV. MEAN FIELD

A. Naive mean field

For large z one may be tempted to use the mean-field approach, in which H_F is replaced by $H_{MF} = \sum_i (-\xi_i \sigma_i^z - B \sigma_i^x)$ where B is determined self-consistently from the equation $B = \sum_j \langle \sigma_j^x \rangle$. At temperature $T = 1/\beta$, the self consistent equation for B obtained at $z \rightarrow \infty$ is:

$$B = z \int d\xi \pi(\xi) \int dJ \rho(J) \frac{B}{\sqrt{\xi^2 + B^2}} \tanh(\beta \sqrt{\xi^2 + B^2}) . \quad (7)$$

At finite temperature there is a transition between a large disorder paramagnetic phase where $B = 0$ is the only solution of this equation, to a ferromagnetic phase characterized by a non-zero field, $B > 0$. The critical temperature T_c is given by:

$$\frac{1}{h} \int_0^h d\xi \frac{\tanh(\xi/T_c)}{\xi} = 1 . \quad (8)$$

At zero temperature this naive mean field approach predicts that the system is always in its ferromagnetic phase.

While this approach is correct when $z = \infty$, its conclusions are qualitatively wrong for any finite z .

B. Bethe-Peierls approximation

The naive mean field prediction that the system is always ferromagnetic at zero T is wrong; the reason is that the mean field approach does not take into account properly the rare events. Rare sites j where the energy $|\xi_j| \ll 1$ can be easily polarized in the x direction, and they play a key role in the establishment of the ferromagnetic order. This effect, which has been first discussed qualitatively in [37], leads to a zero temperature quantum phase transition to a paramagnetic state at a critical value of disorder h_c . In order to study this quantum transition in details, we shall use the quantum version of the cavity method.

V. THE QUANTUM CAVITY METHOD AND ITS PROJECTIONS

A. The RS quantum cavity method

Let us study the transverse-field Ising Hamiltonian (5) on a Bethe lattice defined as a random regular graph. The partition function $Z = \text{Tr} e^{-\beta H_I}$ can be expressed with the Suzuki-Trotter representation. Using M imaginary time steps, we introduce at each time step a decomposition on the eigenvectors of the operators σ_j^x . This describes the system by the classical time trajectory of each spin, $\sigma_i(t) \in \pm 1$, where $t = 1, \dots, M$, and $\sigma_j(t)$ denotes the eigenvalue of σ_j^x at time t . Then

$$Z = \lim_{M \rightarrow \infty} \sum_{\{\sigma_i(t)\}} e^{-\beta H_{ST}} \quad (9)$$

where:

$$H_{ST} = -\frac{1}{M} \sum_t \sum_{(ij)} J_{ij} \sigma_i(t) \sigma_j(t) - \sum_t \sum_i \Gamma_i \sigma_i(t) \sigma_i(t+1) \quad (10)$$

and $\Gamma_i = \frac{1}{2\beta} \log \coth \left(\frac{\beta \xi_i}{M} \right)$

This Hamiltonian acts on spin trajectories $\vec{\sigma}_j = \{\sigma_i(t), t = 1, \dots, M\}$. Each trajectory can be seen as a variable $\vec{\sigma}_j$ taking 2^M possible values, and H_{ST} defines the interaction of these N variables. The crucial point is that this Hamiltonian involves interactions between pairs of trajectories which are neighbours on the Bethe lattice. This is a locally tree-like graph and therefore one can use the cavity method to study it. The RS cavity method for this problem was introduced in [38]. It is obtained from the classical cavity method described in Sect.II B by using spin trajectories instead of Ising spins. Take a branch of the Bethe lattice rooted on spin 0, and define the probability distribution of the time-trajectory of this spin as $\psi_0[\vec{\sigma}_0]$. Define analogously, for each of the K spins i which are the first neighbors of 0 on the rooted tree, their time trajectory as $\psi_i[\vec{\sigma}_i]$. Then one can write the mapping that generates, from $\{\psi_i[\vec{\sigma}_i]\}$, the new $\psi_0[\vec{\sigma}_0]$:

$$\begin{aligned} \psi_0[\vec{\sigma}_0] = C \sum_{\vec{\sigma}_1, \dots, \vec{\sigma}_K} & \psi_1[\vec{\sigma}_1] \dots \psi_K[\vec{\sigma}_K] \\ & \exp \left(\frac{\beta}{M} \sum_t \sum_{(i)} J_{0i} \sigma_0(t) \sigma_i(t) + \beta \sum_t \Gamma_0 \sigma_0(t) \sigma_0(t+1) \right) \end{aligned} \quad (11)$$

The population dynamics method of Sect.II B can be used to study this cavity recursion: one must represent each of the ψ_i by a sample of spin trajectories. This has been done for some

problems in [38,39], but this approach tends to be rather heavy numerically. In particular, in a disordered system like the random transverse-field ferromagnet, the natural order parameter is the distribution of the functions ψ_j when the site j is drawn randomly. This is a rather complicated object which must be represented as a population of populations.

B. The projected cavity mapping

While the exact RS cavity mapping is in principle doable, the difficulty in its numerical resolution may make it difficult to get a clear understanding of the physical results. For this reason one may want to develop approximate versions of it. One such approximation, the projected cavity mapping introduced in [1], consists in using a local distribution $\psi_i[\vec{\sigma}_i]$ which takes the special form, parameterized by one single number B_i :

$$\psi_i[\sigma_i(t)] = C \exp\left(\frac{\beta B_i}{M} \sum_t \sigma_i(t) + \beta \Gamma_i \sum_t \sigma_i(t) \sigma_i(t+1)\right). \quad (12)$$

Injecting this form into (11) we obtain a ψ_0 which does not have the form (12). However one can project it back on a ψ_0 in the right subspace described by (12) as follows. From the obtained ψ_0 one can compute $\langle \sigma_0^x \rangle$ and deduce from it the effective parameter B_0 such that the distribution $C \exp\left(\frac{\beta B_0}{M} \sum_t \sigma_0(t) + \beta \Gamma_0 \sum_t \sigma_0(t) \sigma_0(t+1)\right)$ gives this value of $\langle \sigma_0^x \rangle$.

This projected cavity mapping is actually more easily understood directly in terms of quantum Hamiltonians, without going to the Suzuki-Trotter formalism. One studies the properties of a spin 0 in the rooted graph where one of its neighbors has been deleted, assuming that the K remaining neighbors are uncorrelated. Each of these neighbours, when it is at the root of the subtree obtained by deleting the link to spin 0, is supposed to be described by a Hamiltonian

$$H_i^{cav} = -\xi_i \sigma_i^z - B_i \sigma_i^x \quad (13)$$

The system of spin 0 and its K neighbors is thus described by the local Hamiltonian

$$H_0 = -\xi_0 \sigma_0^z - \sum_{i=1}^K (\xi_i \sigma_i^z + B_i \sigma_i^x + J_{0i} \sigma_0^x \sigma_i^x) \quad (14)$$

By diagonalizing this $2^{K+1} \times 2^{K+1}$ Hamiltonian, one can compute the induced magnetization of spin 0, $m_0 = \langle \sigma_0^x \rangle$. In order for this approach to be self-consistent, this magnetization

should be equal to the one obtained from the Hamiltonian $-\xi_0\sigma_i^z - B_0\sigma_i^x$. This means that B_0 is obtained by solving the equation:

$$\frac{B_0}{\sqrt{\xi_0^2 + B_0^2}} \tanh \beta \sqrt{\xi_0^2 + B_0^2} = m_0 \quad (15)$$

The projected cavity mapping thus uses a single number B_i to describe the trajectory distribution ψ_i . It leads to a mapping which gives the new cavity field B_0 in terms of the K fields B_i on the neighboring spins. This mapping induces a self-consistent equation for the distribution of the B fields, which is the natural order parameter in this context: the paramagnetic phase has $P(B) = \delta(B)$, and the ferromagnetic phase is described by a non-trivial $P(B)$. The population dynamics method can be used to find this distribution.

C. The cavity-mean-field approximation

The projected cavity mapping is numerically much simpler than the full RS cavity method using spin trajectories. It also allows to address a broader range of questions, like those related to the real time dynamics and the spin relaxation, which are not easily accessible within the Suzuki-Trotter formalism^{1,2}. Still its practical use is a bit slow numerically as one must diagonalize the $K + 1$ spin Hamiltonian (14) each time one wants to generate a new field B_0 in the population.

It has turned out useful¹ to use one more step of approximation in order to obtain an explicit mapping, similar to the one found in the classical problem (3). This can be done using a mean field approximation in order to compute the magnetization m_0 from the cavity Hamiltonian (14). In this 'cavity-mean-field approximation', one approximates the cavity Hamiltonian acting on spin 0 by

$$H_0^{cav-MF} = -\xi_0\sigma_0^z - \sigma_0^x \sum_{i=1}^K J_{0i} \langle \sigma_i^x \rangle \quad (16)$$

This implies that $B_0 = \sum_{i=1}^K J_{0i} \langle \sigma_i^x \rangle$, giving the explicit recursion equation relating the B fields:

$$B_0 = \sum_{i=1}^K J_{0i} \frac{B_i}{\sqrt{B_i^2 + \xi_i^2}} \tanh \beta \sqrt{B_i^2 + \xi_i^2}. \quad (17)$$

This recursion induces a self-consistent equation for the distribution $P(B)$ which can now

be written explicitly:

$$P(B) = \int \prod_{i=1}^K [dB_i d\xi_i dJ_{0i} P(B_i) \rho(J_{0i}) \pi(\xi_i)] \delta \left(B - \sum_{i=1}^K \frac{J_{0i} B_i}{\sqrt{B_i^2 + \xi_i^2}} \tanh \beta \sqrt{B_i^2 + \xi_i^2} \right). \quad (18)$$

VI. A SIMPLE TEST OF THE PROJECTED CAVITY RECURSION: THE PURE FERROMAGNET

It is useful to test the validity of the two levels of approximation described above (the projected cavity mapping and the cavity-mean-field approximation) versus precise results using the full numerical sampling of Suzuki-Trotter trajectories. This can be done in the case of a pure ferromagnet in a uniform transverse field, defined by $\rho(J) = \delta(J - 1)$ and $\pi(\xi) = \delta(\xi - h)$. We thus study the problem defined by the Hamiltonian

$$H_{PF} = -h \sum_i \sigma_i^z - \sum_{(ij)} \sigma_i^x \sigma_j^x \quad (19)$$

on a random regular graph where each site has $z = K + 1$ neighbours. The exact cavity study in terms of continuous-time spin trajectories has been done in the case $K = 2$ by [39], we shall use their results as a benchmark in order to test the accuracy of the three levels of approximations:

1: Naive mean field: The Eq.(7) for the spontaneous field B in the x direction becomes:

$$B = (K + 1) \frac{B}{\sqrt{h^2 + B^2}} \tanh(\beta \sqrt{h^2 + B^2}). \quad (20)$$

2: Cavity-mean-field: The recursion relation (17) now becomes a self-consistent equation for the spontaneous field B in the x direction (which is site-independent):

$$B = K \frac{B}{\sqrt{h^2 + B^2}} \tanh(\beta \sqrt{h^2 + B^2}), \quad (21)$$

it differs from the naive mean field only by the replacement $K + 1 \rightarrow K$.

3: Projected cavity mapping: The system of spin 0 and its K neighbors is described by the local Hamiltonian

$$H_0 = -h \sigma_0^z - \sum_{i=1}^K (h \sigma_i^z + B \sigma_i^x + \sigma_0^x \sigma_i^x) \quad (22)$$

The self-consistent equation for the spontaneous field B in the x direction is given by

$$m_0 = \frac{\text{Tr}(\sigma_0^x e^{-\beta H_0})}{\text{Tr} e^{-\beta H_0}} = \frac{B}{\sqrt{h^2 + B^2}} \tanh \beta \sqrt{h^2 + B^2}. \quad (23)$$

These traces involve matrices of size 2^{K+1} , they are easily computed numerically when K is not too large.

The phase diagram obtained with these three approximations is plotted in Fig.3, and compared to the exact one of [39]. The projected cavity mapping gives a rather precise approximation of the phase diagram, much better than the one obtained by naive mean field or by the well known static approximation (see [39]). A slightly better result can be obtained by using the parameterized form (12) variationally inside the Bethe free energy⁴⁶.

One may also use the cavity method as a mean field approximation to study the finite dimensional problem. It turns out that it is able to locate the transition point rather accurately. For a three dimensional case, the simulations through a cluster Monte-Carlo method of the Suzuki-Trotter formulation⁴⁰ gives a zero-temperature transition occurring at $h_c = 5.16$. The projected cavity mapping (with $K = 5$) gives $h_c = 5.28$, and the cavity-mean-field gives $h_c = 5.00$. In two dimensions, the numerical result of [32,40] is $h_c = 3.04$, the projected cavity mapping (with $K = 3$) gives $h_c = 3.22$, and the cavity-mean-field gives $h_c = 3.00$.

VII. PHASE DIAGRAM OF THE RANDOM TRANSVERSE-FIELD FERRO-MAGNET

Let us apply the cavity-mean-field approximation to the random transverse-field ferromagnet. The whole problem reduces to finding the distribution of fields $P(B)$ which solves the self-consistent equation (18). It turns out that the solution of this equation is more subtle than the one of seemingly similar equations obtained in the classical case.

In order to understand the properties of this solution, it is useful to go back to the cavity mapping (17). Let us iterate this mapping $L \gg 1$ times on the Bethe lattice. For L finite and $N \rightarrow \infty$ the corresponding graph is just a rooted tree with branching factor K at each node and depth L . The field B_0 at the root is a function of the K^L fields on the boundary. In order to see whether the system develops a spontaneous ferromagnetic order, we study the value of B_0 in linear response to infinitesimal fields $B_i = B \ll 1$ on the boundary spins.

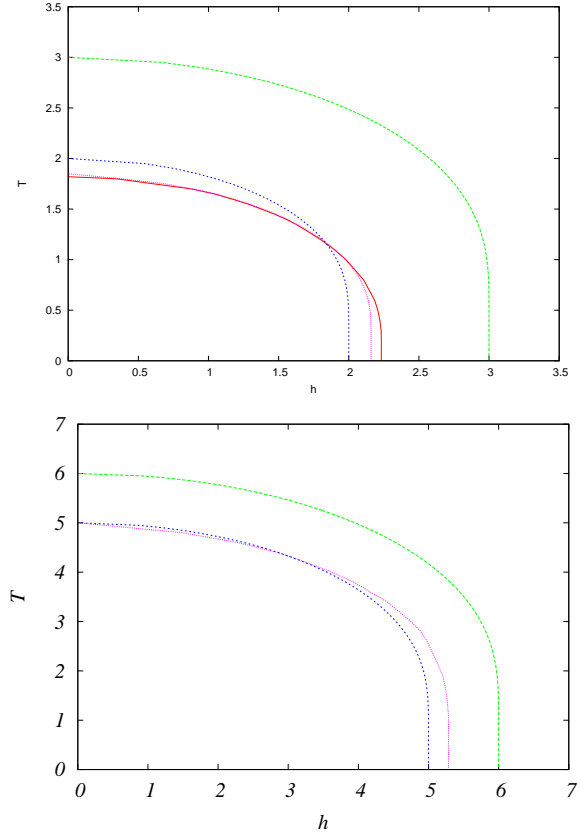


FIG. 3. **Top:** The phase diagram of the ferromagnet in a transverse field, on a Bethe lattice with $K + 1 = 3$ neighbours per spin. The plot shows the critical temperature versus transverse field, separating the low- T ferromagnetic region from the high- T paramagnetic one. The full red curve is the exact result obtained by continuous time spin trajectory population dynamics³⁹. The green long-dashed curve is the naive mean field result. The blue dashed line is the result from the cavity-mean-field approximation. The dotted purple curve is the result obtained from the projected cavity mapping. **Bottom:** Same plots with $K + 1 = 6$ (without the exact result), showing that the approximation going from the projected cavity mapping to the cavity-mean-field improves at larger K , as expected, and becomes rather accurate already for this moderate value of K .

This is given by

$$B_0/B = \Xi \equiv \sum_P \prod_{k \in P} \left[\frac{J_k \tanh(\beta \xi_k)}{\xi_k} \right]. \quad (24)$$

where the sum is over all paths going from the root to the boundary, and the product $\prod_{k \in P}$ is over all edges along the path P .

A. Phase transition and directed polymers

The response Ξ is nothing but the partition function for a directed polymer in a random medium (DPRM) on a tree, where there exists on each edge k of the tree a random energy E_k given by $e^{-E_k} = J_k(\tanh(\beta\xi_k)/\xi_k)$ and the temperature of the polymer has been set equal to one. The random energies are independent identically distributed random variables. We need to compute the large L behavior of Ξ . As Ξ is a partition function, this is naturally characterized by the free energy

$$\Phi = \lim_{L \rightarrow \infty} (1/L) \ln \Xi . \quad (25)$$

If $\Phi < 0$ the effect of a small boundary field decays with distance: the spin system is paramagnetic. If $\Phi > 0$ it is ferromagnetic.

The general method for computing Φ in DPRM on trees has been developed by Derrida and Spohn⁴¹. Their solution can be expressed in terms of the convex function

$$f(x) = \frac{1}{x} \ln \left[K \int dJ \rho(J) \int d\xi \pi(\xi) \left(\frac{J \tanh(\beta\xi)}{\xi} \right)^x \right] . \quad (26)$$

Let us denote by $x = m$ the value of $x \in [0, 1]$ where this function reaches its minimum. The free energy of the DP is then $\Phi = f(m)$. The phase transition line in the (h, T) plane separating the ferromagnetic from the paramagnetic phase is thus obtained by solving the equation $f(m) = 0$.

In the case of the random transverse-field ferromagnet one obtains

$$f(x) = \frac{1}{x} \ln \left[\frac{K^{1-x}}{1+x} \right] + \log \frac{2}{T} + \frac{1}{x} \log \left[\frac{T}{h} \int_0^{h/T} du \left(\frac{\tanh(u)}{u} \right)^x \right] , \quad (27)$$

from which one deduces the following phase diagram (see Fig.4):

- When the field h is smaller than a value h_R the phase transition line is given by $f(1) = 0$. This gives back the naive mean field result of (8): $h = \int_0^{h/T_c} du \tanh(u)/u$. The value h_R , and the corresponding value $T_R = T_c(h_R)$, are obtained by solving the pair of equations $f(1) = 0$, $f'(1) = 0$.
- When $h > h_R$, the phase transition is given by solving the equations $f(m) = 0$, $f'(m) = 0$. In this regime the solution is at $m < 1$. This low temperature, large disorder part of the phase transition line departs from the naive mean field

prediction. In particular, at variance with the naive mean field result, one finds that there exists a zero temperature quantum phase transition at a critical disorder h_c . This is obtained using the zero-temperature limit of f :

$$f_0(x) = \frac{1-x}{x} \ln K - \frac{1}{x} \log(1-x^2) - \log\left(\frac{h}{2}\right), \quad (28)$$

and solving the two equations $f_0(m) = f'_0(m) = 0$. Fig.5 shows h_c as function of K . In the large K limit h_c diverges, giving back the naive mean field result. However this divergence is very slow: one finds that $m \sim 1 - 1/\log K$ and $h_c \sim e \log K$.

The phase transition line has two parts: a small-disorder part on the left of the point R with coordinates (h_R, T_R) , and a large-disorder part on the right of this point. The properties of these two regimes of the transition are very different. In order to understand this difference, it is useful to give a closer look at the DPRM problem using the replica method, as was first done in [42]. The DP partition function Ξ , defined in (24), depends on the random quenched variables J_n, ξ_n . To compute the value of $\log \Xi$ for a *typical* sample one needs to do a quenched average of $\log \Xi$ over these random variables, denoted by $\overline{\log \Xi}$. As a first step one might try to approximate it by the annealed average $\log \overline{\Xi}$. This gives precisely the naive-mean field result. To go beyond this ‘annealed approximation’ one can introduce replicas, using $\overline{\ln \Xi} = \lim_{n \rightarrow 0} (\overline{\Xi^n} - 1)$. The average of Ξ^n is obtained by a sum over n paths,

$$\overline{\Xi^n} = \sum_{P_1, \dots, P_n} \prod_{a=1}^n \left[\prod_{k \in P_a} \left(J_k \frac{\tanh(\beta \xi_k)}{\xi_k} \right) \right]. \quad (29)$$

One can then proceed by testing various hypotheses concerning the structure of the paths which dominate the replicated partition function (29):

- In the so-called replica symmetric (RS) hypothesis one assumes that the leading contribution to (29) comes from non-overlapping paths. This gives

$$\overline{\Xi^n} = \exp(Ln f(1)) = (\overline{\Xi})^n. \quad (30)$$

The RS hypothesis is equivalent to the annealed approximation in this case.

- The so-called one step replica-symmetry-breaking (1RSB) hypothesis assumes that the leading contribution to (29) comes from patterns of n paths which consist of n/m

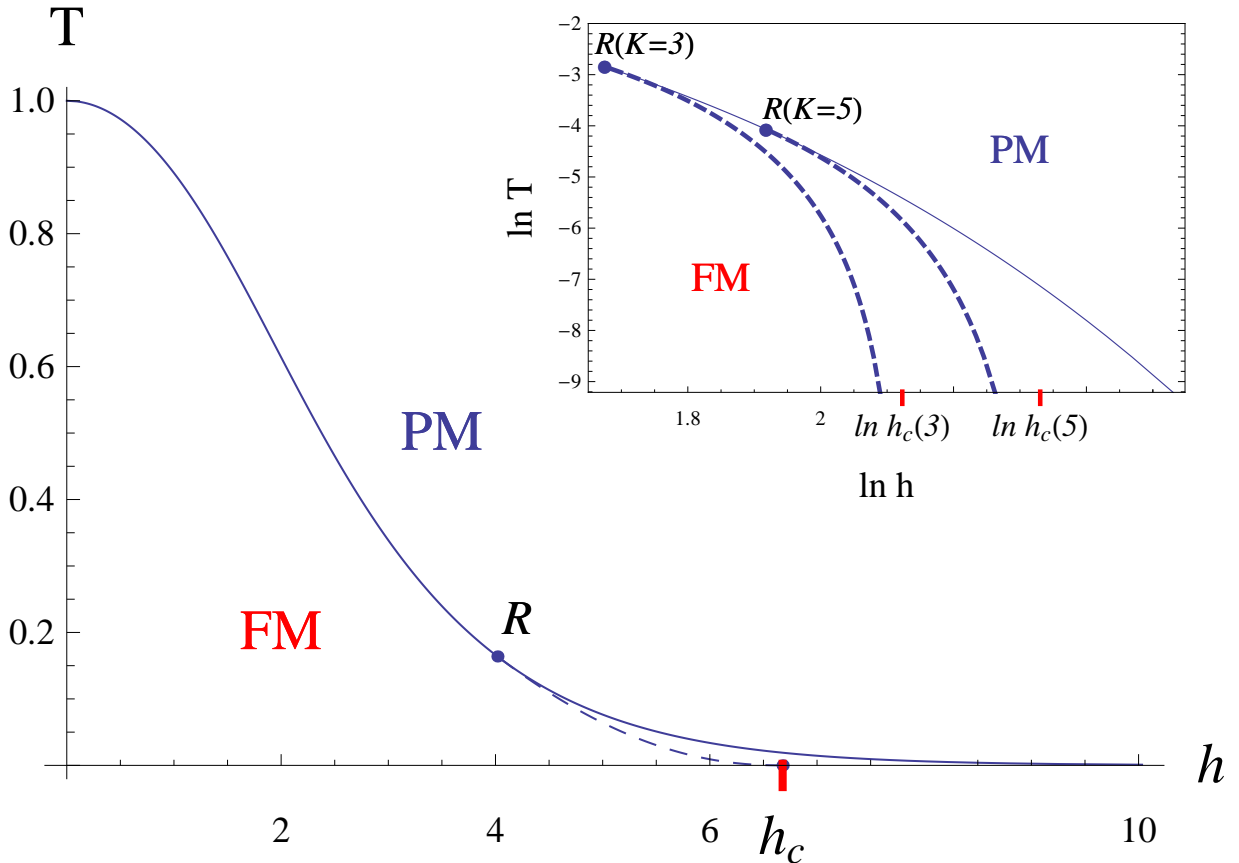


FIG. 4. Phase diagram of the quantum ferromagnet in a random transverse field, as found with the RS cavity method, in the plane of the disorder strength h and the temperature T . The RS transition line (solid) is determined by the condition on the convex function: $f(x = 1, T, h) = 0$, and separates the ferromagnetic (FM) state ($f(x = 1, T, h) < 0$) from the paramagnetic (PM) state ($f(x = 1, T, h) > 0$). The point R on the RS line corresponds to the minimum of the convex function: $f'_x(x = 1, T, h) = 0$. It is the beginning of the RSB transition line, determined by the minimum of the convex function in the RSB ($x^* < 1$) phase: $f(x^*, T, h) = 0$ and $f'_x(x^*, T, h) = 0$. The inset shows details of the RSB lines in the cases $K = 3$ and $K = 5$. The critical values of disorder $h_c(K)$, at which the zero-temperature quantum phase transition to the paramagnetic phase happens, for the two connectivity numbers K are: $h_c(K = 3) = 8.36$ and $h_c(K = 5) = 10.28$.

groups of m identical paths, where the various groups go through distinct edges. This gives:

$$\overline{\Xi^n} = \exp(Ln f(m)) \quad (31)$$

where $f(x)$ is the function introduced in (27). In the replica limit $n \rightarrow 0$, the parameter

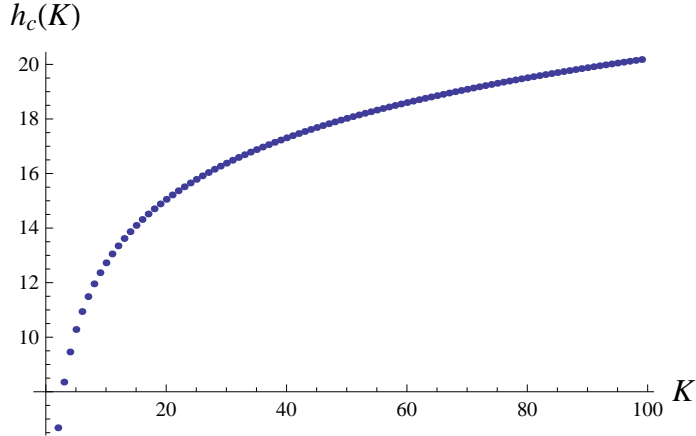


FIG. 5. The critical value of disorder $h_c(K)$, as a function of the connectivity number K .

m should belong to the interval $[0, 1]$. It turns out that one should minimize the function $f(m)$ over $m \in [0, 1]$ (the fact that one should minimize f , and not maximize it as one would have thought naively, is a well-known aspect of the replica method⁴³). The low-temperature large-disorder part of the phase transition line corresponds to this 1RSB solution.

B. Replica symmetry broken phase of the polymer and Griffiths phase of the ferromagnet

This replica solution of our DPRM, with a RS phase at small disorder and a 1RSB phase at large disorder, fully agrees with the original travelling wave solution of [41]. So the point R on the paramagnetic-ferromagnetic transition line of the quantum random transverse-field ferromagnet corresponds to a 1RSB transition in the auxiliary DPRM problem. This is a glass transition of the polymer, similar to the one found in the random energy model^{44,45}, where the measure on the paths condenses on a finite number of paths. A useful order parameter to describe this transition is

$$Y = \frac{1}{\Xi^2} \sum_P \prod_{k \in P} \left[\frac{J_k \tanh(\beta \xi_k)}{\xi_k} \right]^2. \quad (32)$$

This is nothing but the sum $\sum_P w_P^2$ where w_P is the relative weight of path P in the measure (24). Its inverse gives a measure of the effective number of paths contributing to Ξ . In the RS phase one finds that Y vanishes in a typical sample. This can be understood from the

fact that the DPRM partition function gets a contribution from a large number of paths (diverging in the large L limit). In fact the DPRM problem has a finite entropy in this RS phase. On the contrary, in the 1RSB phase one finds that Y is finite and fluctuates strongly from sample to sample. For instance, its first moments are given by [7]:

$$\overline{Y} = 1 - m \quad ; \quad \overline{Y^2} = \frac{1}{3}(1 - m) + \frac{2}{3}(1 - m)^2, \quad (33)$$

and the entropy density of the polymer vanishes in this whole 1RSB phase.

The DPRM problem is an auxiliary construction used to study the phase transition in the original problem of the random transverse field ferromagnet. So the natural question is: what are the consequences of the 1RSB transition in the DPRM concerning the original quantum spin system? Let us go back to (24), which connects the two problems. We consider a large tree of length $L \gg 1$. The condensation of the paths in the DPRM means that, if a small field is applied to the boundary, the value of the effective field B_0 on the root is dominated by a finite number of paths to the boundary. So the root spin feels the effect of only a finite number of the boundary spins. The physics is dominated by rare events: rare boundary spins have a dominant influence of the central spin, and it is building up on these rare events that the system can or cannot develop a long range ferromagnetic order. This is very similar to the Griffiths phase, found originally in the one-dimensional case²⁶, and argued to be present at least in low-dimensional systems. It is interesting to see that we find here a similar rare-event dominated phase, using the mean-field type Bethe approximation which is valid in the opposite limit of large connectivity, $K \gg 1$. The next subsections will give a more detailed discussion of the connections between the results obtained with the cavity method and those known, or conjectured, for finite-dimensional problems. Let us first summarize the main observables that are accessible using the cavity method.

One can study the practical consequences effect of the rare events on both sides of the phase transition, in the neighborhood of the phase transition line, on the right of point R. The study of [2] has discussed these effects in the context of the superconductor-insulator transition. It is easy to translate them to the present situation of the ferromagnetic-paramagnetic transition.

- In the ferromagnetic phase the order parameter (here we use as order parameter the typical local magnetic field B_{typ} in the z direction, obtained as $B_{typ} = \exp(\overline{\log Z})$) has an anomalous scaling and distribution. Imagine one enters the ferromagnetic phase

at a given temperature T by varying the disorder h . At large enough temperature the scaling is $B_{typ} \sim \sqrt{h_c - h}$, as one expects in a mean field system. Then lowering the temperature there is a region above T_R where the scaling is $B_{typ} \sim (h_c - h)^{a(T)}$. The exponent $a(T)$ diverges when $T \rightarrow T_R$. In the 1RSB regime, i.e. for $T < T_R$, the typical field has an essential singularity in $e^{C/(h_c - h)}$. In this regime the distribution of the local order parameter has a power law tail B_{typ}^m / B^{1+m} . As $m < 1$, the average order parameter is divergent.

- In the paramagnetic phase the local susceptibility fluctuates strongly from site to site and nonlinear effects are crucial. Consider the system in a very small uniform magnetic field B_{ext} and look at the local order parameters B_i induced by this external field. The typical value of B_i scales linearly with B_{ext} , but the moments $\overline{B^x}$ with $x > m$, and in particular the mean \overline{B} , are divergent at the level of the linear response to h : they behave non-linearly, as $\overline{B^x} \sim C B_{ext}^m$. The distribution of the local susceptibilities $\chi_i = B_i / B_{ext}$ has a power law tail $P(\chi) \sim C / \chi^{1+m}$.

C. The one-dimensional case

The one-dimensional RTFF is the best understood case. The strong disorder decimation procedure of Ma-Dasgupta-Hu, developed by Fisher²⁶, becomes exact at the transition point because of the existence of an infinite disorder fixed point. It can also be checked versus alternative methods like the mapping of the problem to free fermions^{28,29}, and the exact solution of McCoy and Wu²⁵. A large corpus of results has been obtained by these methods, concerning the scaling behaviour and the Griffiths phase. The strong disorder decimation has turned out to be useful in a broad range of problems³⁰.

Let us mention only some aspects of the physics of the one-dimensional case for which one can draw a comparison between the exact results and those of the cavity method. The exact analysis of the problem has shown that the zero-temperature critical point is located at the width of the random transverse field $h = h_c$ such that $\overline{\log \xi} = \overline{\log J}$, or explicitly: $\int d\xi \pi(\xi) \log \xi = \int dJ \rho(J) \log J$. In our case this gives $h_c = 2$. At the critical point the system displays activated dynamical scaling: the scaling exponent z_c , relating the characteristic time scale τ to the characteristic length scale ξ through $\tau = C \xi^{z_c}$, is formally infinite. Instead the scaling is $\log \tau = C \xi^\psi$. The Griffiths phase can be studied close to

the critical point. Defining $\delta = (\overline{\log h} - \overline{\log J}) / (\text{var}[\log h] + \text{var}[\log J])$, where the overline denotes the average and var denotes the variance, this exponent has been shown to behave as $z(\delta) \sim 2/\delta + C$, where C is a non-universal constant. This exponent $z(\delta)$ also appears in the singular response of the system to an external magnetic field H : in the paramagnetic phase, the linear susceptibility diverges, and the magnetization behaves as $M \sim |H|^{1/z(\delta)}$.

Let us now present the results of the cavity method described in the previous subsection. The one-dimensional case is obtained by taking $K = 1$. Actually it is useful to keep $K = 1 + \epsilon$ at intermediate steps of the computation, and take the $\epsilon \rightarrow 0$ limit in the end. At zero temperature, the minimum of the function $f(x)$ is obtained at $x = m = \sqrt{\epsilon}$, and the critical value of h , obtained by solving $f(m) = 0$, is $h_c = 2(1 + 2\sqrt{\epsilon})$. When $\epsilon \rightarrow 0$, h_c goes to 2 which is the exact result, and $m \rightarrow 0$. The exponent m is the one that controls the decay of the local field distribution (which goes as $B^{-(1+m)}$), and the distribution of local susceptibilities. From the analysis of [2], this exponent m controls the response to a uniform external field, $M \sim |H|^m$. So one should identify $m = 1/z(\delta)$. At the critical point we have found $m \rightarrow 0$. This agrees with $z_c = \infty$ and the activated scaling behaviour. Let us now study the behaviour close to the critical point, at $h = h_c(1 + y)$. At $K = 1$ (or $\epsilon = 0$), one obtains $m = y + O(y^2)$. So the prediction of the cavity method is $z = 1/y$. It turns out that, when expressed in terms of the distance to the critical point δ , this gives the exact result $z = 1/(2\delta)$.

The quantum cavity method is exact in one dimension, if one uses the full mapping of spin trajectories given in (11). It must thus reproduce the exact results. What we have seen is that even the simpler cavity-mean-field approximation gives a fair description of the problem, including the exact location of the critical point, the activated dynamical scaling, and the correct value of z close to the critical point. Actually it gives the exact correlation even for a finite length problem, as we now show.

Consider a chain described by the Hamiltonian

$$H_{1d} = - \sum_{n=1}^L \xi_n \sigma_n^z - \sum_{n=1}^{L-1} J_n \sigma_n^x \sigma_{n+1}^x . \quad (34)$$

In order to see the onset of long-range order, one can fix that the end-spin σ_L is in the eigenstate of σ_L^x with eigenvalue +1, fix $\xi_L = 0$, and compute the so-called 'surface' magnetization at the other end-point in the ground state $m_1 = \langle 0 | \sigma_1^x | 0 \rangle$. By using the Jordan-Wigner trans-

formation of this problem to free fermions, Iglói and Rieger have shown that²⁹:

$$m_1 = \left[1 + \sum_{n=1}^{L-1} \left(\prod_{r=1}^n \frac{\xi_r}{J_r} \right)^2 \right]^{-1/2} \quad (35)$$

This formula, which is exact for a finite system, can then be used to study the critical behavior of the problem. For instance, [29] shows how to deduce from this formula several interesting physical properties: the typical and the average surface magnetization differ, the average critical magnetization scales like $L^{-1/2}$, the exponent β_s giving the surface magnetization close to the critical point is equal to $\beta_s = 1$, the correlation length exponent ν is equal to $\nu = 2$.

Let us now use the cavity-mean-field method on this one-dimensional problem. At zero temperature, formula (17) gives the recursion

$$B_{n-1} = J_{n-1} \frac{B_n}{\sqrt{B_n^2 + \xi_n^2}}, \quad (36)$$

which should be initialized with $B_L = \infty$, $\xi_L = 0$. It is easy to see that, iterating the mapping (36), and computing $m_1 = B_1/\sqrt{B_1^2 + \xi_1^2}$, one obtains the exact formula (35). Therefore the cavity method, even using the simplified, mean-field mapping, gives the exact value of the surface magnetization, also for a finite system. Its predictions thus agree with the known results, including the values of the exponents β_s and ν .

D. Dimensions two and above

There is no exact solution of the two-dimensional RTFF problem. This problem has been studied mostly using the strong-disorder decimation procedure^{33,35,36}, and also using cluster Monte-Carlo simulations of the 2+1 dimensional problem obtained in the Suzuki-Trotter representation^{31,32}. These works have mostly used a different normalization, in which $\rho(J)$ is the uniform distribution on $J \in [0, 1]$, and $\pi(\xi)$ is uniform on $[0, h]$. In this subsection we shall thus adopt this other normalization. The results obtained both by decimation and by Monte-Carlo indicate that the situation is similar to the one-dimensional case. In particular, the exponent z_c is found to diverge, and $1/z(\delta)$ goes to zero as $\delta \rightarrow 0$. In order to obtain an analytic approximation to this two-dimensional problem, one can repeat the cavity study on the Bethe lattice with $K = 3$.

Within the cavity-mean-field approximation, the function $f(x)$ is found to be

$$f(x) = \frac{1}{x} \log 3 - \frac{1}{x} \log(1 - x^2) - \log h. \quad (37)$$

It is minimum at $x = m = .679$, and the critical value of the field, obtained from $f(m) = 0$, is found to be $h_c = 12.53$. This result disagrees with the strong-disorder decimation, and with the Monte-Carlo, in two aspects: i) the value of h_c (with the Monte-Carlo it is found^{31,32} around $h_c \sim 4.2$, with the decimation it is found³⁴⁻³⁶ around $h_c \sim 5.3$), ii) most importantly, the fact that the value of m found in the cavity method does not go to zero at the transition.

One may wonder to what extent these results depend on the approximation. If instead of doing the cavity-mean-field approximation one uses the more accurate projected cavity mapping, the value of h_c is changed to $h_c \sim 7.5$, but the value of m is unchanged. This is seen from Fig.6, which shows the inverse of the typical value of the local field B , measured as $\exp(-\overline{\ln B})$, plotted versus $(h_c/h)^m - 1$. The prediction of [2] is that the inverse of the typical value of B should go to zero linearly in $(h_c/h)^m - 1$. Both data sets, obtained from the cavity-mean-field approximation and from the projected cavity mapping, find this behaviour, but the values of h_c in both data sets are distinct (respectively $h_c = 12.53$, as predicted from our analytic study with the DPRM, and $h_c = 7.5$, found from the fit).

The conclusion is that, while the non-universal critical value h_c depends quite a lot of the approximation used in the cavity method, the value of m does not, and the statement that $m \neq 0$ at the transition seems to be a solid result for the problem on the Bethe lattice with any connectivity $K + 1 \geq 3$. Notice that this result still implies that there is a strong hierarchy of local magnetic fields: the average field diverges, and so does the average susceptibility. But it is not an infinitely strong hierarchy as happens when $m = 0$. It should be noticed that our best cavity analysis, using projected cavity mapping, still involves some approximation, and it would be interesting to carry out the full Suzuki-Trotter trajectory mapping in order to get the exact solution for the Bethe lattice. At present, our approximate treatment gives $m > 0$ at the transition for the Bethe lattice problem a result which disagrees with a recent study from strong disorder decimation³⁶. It should be noticed that our cavity approximations should become exact in the large K limit of the Bethe lattice. Assuming that the result $z_c \neq \infty$ is correct for the Bethe lattice, this raises the question of the existence and value of a critical dimension above which the finite dimensional problems have $z_c \neq \infty$.

It would thus be interesting to revisit the numerical results in $d = 2$ and $d > 2$, and on

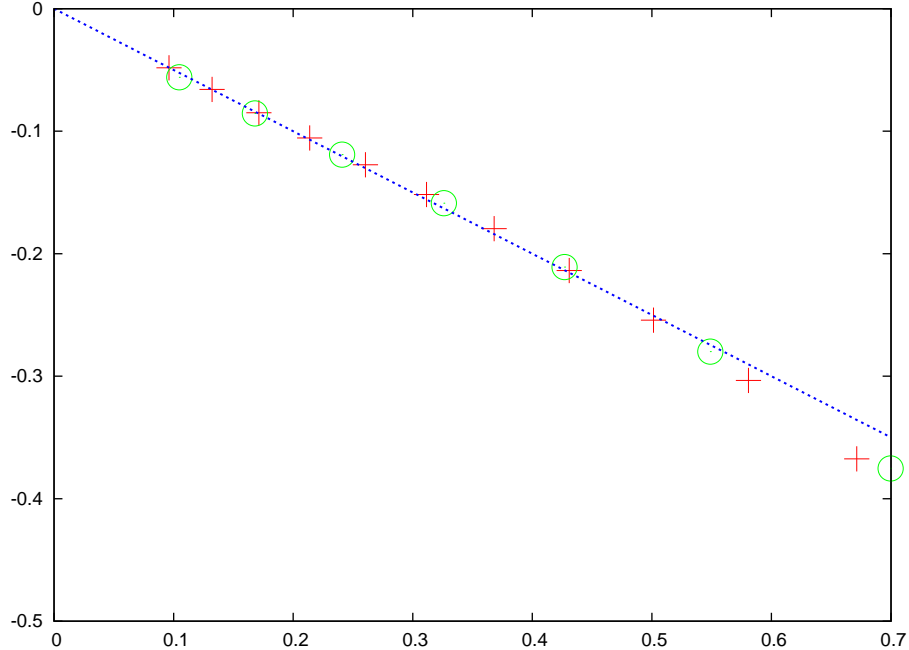


FIG. 6. Phase transition in the RTFF model with $K = 3$, a uniform distribution of couplings J on $[0, 1]$, and a uniform distribution of fields ξ on $[0, h]$. The typical value of the local field B , measured as $\exp(-\overline{\ln B})$, is plotted versus $(h_c/h)^m - 1$. The crosses are obtained with the cavity-mean-field approximation and the choice $h_c = 12.53$ obtained from the analytic study of the DPRM problem, which predicts a linear dependence $\exp(-\overline{\ln B}) = C[(h_c/h)^m - 1]$. The circles are obtained with the projected cavity mapping, and a fitted value $h_c = 7.5$. In both cases the exponent m is the one found from the DPRM analysis, $m = 0.679$. The straight line is a guide to the eye.

the Bethe lattice, giving $m = 0$ at the transition. Concerning the Monte-Carlo approach, let us point out in particular that the RSB effects happen at very low temperature, but they completely change the physics of the problem (for the problem with $K = 3$ and uniform couplings on $[0, 1]$, we have found with the cavity-mean-field approximation that the RSB transition point on the ferromagnetic-paramagnetic transition line occurs at $T_R \sim 0.087$). So the numerical results obtained by extrapolation from a not-very-low temperature to $T = 0$ might be questionable.

VIII. SUMMARY

We have proposed here a well defined mean-field scheme to study quantum ferromagnets in random transverse fields. This scheme consists in studying the problem on a random

regular graph with fixed connectivity $K + 1$. The problem at finite z is qualitatively distinct from the infinite z case, described by the naive mean field theory. It has a zero temperature quantum phase transition at a finite critical value of the width of the distribution of random transverse fields.

The phase diagram has been studied by the RS quantum cavity method. A full study would involve a complicated population dynamics in terms of imaginary time spin trajectories, which would be extremely costly in terms of computing efforts. Instead we have resorted to a simple approximation, the cavity mean-field approximation, which parameterizes the imaginary time spin trajectories by a single number, a local cavity longitudinal field. Within this approximation, the RS cavity method becomes a simple recursion relation on these local fields. While this recursion looks structurally similar to the one found in classical spin systems, its physical content is very different. When one iterates L times the linearized recursion describing the phase transition, one obtains the partition function for a classical directed polymer in a random medium on a tree. This problem has a glass transition. The small disorder phase of the polymer describes the high temperature part of the ferromagnetic to paramagnetic phase transition, which is identical to what one gets in the naive mean field approach. The large disorder phase of the polymer describes the lower temperature part of the ferromagnetic to paramagnetic phase transition, which has a completely different behavior. This glass phase of the polymer, which displays replica symmetry breaking, actually describes the Griffiths phase of the quantum spin system in the neighborhood of its quantum phase transition. The results obtained with the cavity analysis fully agree with the known behaviour of the system in one dimension. On Bethe lattices with connectivity $K + 1 \geq 3$, we find a Griffiths phase, as in one dimension, but the critical point is not an infinite disorder fixed point: the exponent m which governs the tail of the local field distribution does not vanish at the transition, meaning that the critical exponent z does not diverge. it would be interesting to know if there is a critical dimension of finite dimensional problems beyond which such a behaviour appears.

One should be aware of the fact that we have been using here a RS cavity method for the quantum spin system. Nevertheless, even within this RS method, the cavity equations map onto a classical problem which exhibits RSB. It would be very interesting, in particular when applying this formalism to spin glasses, to study the effect of RSB within the quantum cavity method itself.

ACKNOWLEDGMENTS

The results in Sect.VII are straightforward consequences of the works [^{1,2}] in collaboration with L. Ioffe and M. Feigelman. MM wants to thank them, and also G. Biroli, D. Huse, G. Semerjian, M. Tarzia and F. Zamponi for useful exchanges. The $K = 2$ graph in Fig. 3 was originally computed by F. Zamponi, who has kindly given us the data of the exact result obtained by the continuous time spin trajectory population dynamics. The grant Triangle de la Physique 2007-36 has supported the work of OD and our collaboration with L. Ioffe.

REFERENCES

- ¹ L.B. Ioffe and M. Mézard, Phys. Rev. Lett. **105**, 037001 (2010).
- ² M.V. Feigel'man, L.B. Ioffe and M. Mézard, arXiv:1006.5767.
- ³ M.Mézard, G. Parisi and M. A. Virasoro, Europhys. Lett. **1**, 77 (1985).
- ⁴ D. Sherrington and S. Kirkpatrick, Phys. Rev. Lett. **35**, 1792 (1975).
- ⁵ G. Parisi, J. Phys. A **13**, 1101 (1980); G. Parisi, J. Phys. A **13**, L115 (1980).
- ⁶ G. Parisi, Phys. Rev. Lett. **50**, 1946 (1983).
- ⁷ M. Mézard, G. Parisi, N. Sourlas, G. Toulouse and M.A. Virasoro, Journal de Physique **45**, 843 (1983).
- ⁸ M. Mézard, G. Parisi and M.A. Virasoro, J. Physique Lett. **46** (1985) L217.
- ⁹ M. Talagrand, C. R. Acad. Sci. Paris, Ser. I 337 (2003).
- ¹⁰ F. Guerra, Comm. Math. Phys. **233**, 1 (2003).
- ¹¹ S.F. Edwards and P.W. Anderson, J. Phys. F **5**, 965 (1975).
- ¹² J.R.L. de Almeida and D. Thouless, J. Phys. A **11**, 983 (1978).
- ¹³ D.J. Thouless, P.W. Anderson and R.G. Palmer, Phil. Mag. **35**, 593 (1977).
- ¹⁴ A.J. Bray and M. Moore, J. Phys. C **13**, L469 (1979).
- ¹⁵ D.J. Thouless, Phys. Rev. Lett. **6**, 1082 (1986).
- ¹⁶ J.T. Chayes, L. Chayes, J. P. Sethna and D.J. Thouless, Commun. Math. Phys. **106**, 41 (1986).
- ¹⁷ M. Mézard and A. Montanari, J. Stat. Phys. **124**, 1317 (2006).

- ¹⁸ L Viana and A. J. Bray, J. Phys. C **18**, 3037 (1985).
- ¹⁹ M. Mézard and G. Parisi, Europhys. Lett. **3** (1987) 1067.
- ²⁰ I. Kanter and H. Sompolinsky, Phys. Rev. Lett. **58**, 164 (1987).
- ²¹ M. Mézard and G. Parisi, Eur. Phys. J. B **20** (2001) 217.
- ²² For a recent review, see M. Mézard and A. Montanari, *Information, Physics, and Computation*, Oxford University Press (2009).
- ²³ R. Abou-Chacra, P.W. Anderson and D.J. Thouless, J. Phys. C **6**, 1734 (1973).
- ²⁴ S. Sachdev, *Quantum Phase Transitions*, Cambridge University Press (2000).
- ²⁵ B.M. MacCoy and T.T. Wu, Phys. Rev. **176**, 631 (1968).
- ²⁶ D.S. Fisher, Phys. Rev. Lett. **69**, 534 (1992); Phys. Rev. B **50**, 3799 (1994).
- ²⁷ S. Ma, C. Dasgupta and C. Hu, Phys. Rev. Lett. **43**, 1434 (1979); C. Dasgupta and S. Ma, Phys. Rev. B **22**, 1305 (1980).
- ²⁸ A.P. Young and H. Rieger, Phys. Rev. B **53**, 8486-8498 (1996).
- ²⁹ F. Iglói and H. Rieger, Phys.Rev. **57**, 11404 (1998).
- ³⁰ For a review, see: F. Iglói and C. Monthus, Phys. Rep. **412**, 277 (2005).
- ³¹ C. Pich et al., Phys. Rev. Lett. **81**, 5916 (1998).
- ³² H. Rieger and N. Kawashima, Eur. Phys. J. B **9**, 233 (1999).
- ³³ O. Motrunich, S.-C. Mau, D. A. Huse and D.S. Fisher, Phys. Rev. B **61**, 1160 (2000).
- ³⁴ R. Yu, H. Saleur and S. Haas, Phys. Rev. B **77**, 140402 (2008).
- ³⁵ I. A. Kovács and F. Iglói, Phys. Rev. B **82**, 054437 (2010).
- ³⁶ I. A. Kovács and F. Iglói, arXiv:1010.2344v1.
- ³⁷ M. Ma, B. Halperin and P. Lee, Phys. Rev. B **34**, 3136 (1986).
- ³⁸ C. Laumann, A. Scardicchio and S. L. Sondhi Phys. Rev. B **78**, 134424 (2008).
- ³⁹ F. Krzakala, A. Rosso, G. Semerjian and F. Zamponi, Phys. Rev. B **78**, 134428 (2008).
- ⁴⁰ H. W. J. Blöte and Y. Deng, Phys. Rev. E **66**, 066110 (2002).
- ⁴¹ B. Derrida and H. Spohn J. Stat. Phys. **51**, 817 (1988).
- ⁴² J. Cook and B. Derrida J. Phys. A **23**, 1523 (1990).
- ⁴³ M. Mézard, G. Parisi and M. Virasoro “Spin Glass Theory and Beyond”, World Scientific, Singapore (1987).
- ⁴⁴ B. Derrida, Phys. Rev. B **24**, 2613 (1981).
- ⁴⁵ D.J. Gross and M. Mézard, Nucl. Phys. B **240**, 431 (1984).

⁴⁶ F. Zamponi, private communication.